Materials Transactions, Vol. 54, No. 3 (2013) pp. 405 to 408

Compression Properties of Al/Al–Si–Cu Alloy Functionally Graded Aluminum Foam Fabricated by Friction Stir Processing Route

Yoshihiko Hangai[1], Kousuke Saito[1,*], Takao Utsunomiya[2], Soichiro Kitahara[3], Osamu Kuwazuru[4] and Nobuhiro Yoshikawa[5]

[1]*Graduate School of Engineering, Gunma University, Kiryu 376-8515, Japan*
[2]*Research Organization for Advanced Engineering, Shibaura Institute of Technology, Saitama 337-8570, Japan*
[3]*Hokudai Co., Ltd., Abira 059-1434, Japan*
[4]*Graduate School of Engineering, University of Fukui, Fukui 910-8507, Japan*
[5]*Institute of Industrial Science, The University of Tokyo, Tokyo 153-8505, Japan*

Functionally graded (FG) aluminum foam containing A1050 pure aluminum and ADC12 aluminum alloy was fabricated. The FG foam has the potential for its location of deformation to be controlled. Moreover, a FG foam with plateau regions and stresses corresponding to those of the uniform A1050 and ADC12 foams was obtained. [doi:10.2320/matertrans.M2012376]

(Received November 8, 2012; Accepted December 14, 2012; Published February 1, 2013)

Keywords: *cellular materials, functionally graded materials (FGM), friction stir welding*

1. Introduction

Al foam is a promising material for automobile components to improve both fuel efficiency and the safety of passengers owing to its light weight and high energy absorption.[1,2] Functionally graded (FG) Al foam, in which the properties vary with the position, is expected to improve the performance of Al foam. There are several processing routes for fabricating FG Al foam, such as the casting route replication process,[3–6] powder metallurgy route replication process,[7] syntactic foam process[8] and precursor process.[9,10] In these processes, the variation of properties is achieved through position-dependent pore structures.

Recently, a friction stir processing (FSP) route for fabricating the precursor of Al foam has been developed.[11] FSP was developed from the basic principles of friction stir welding (FSW), which is a solid-state bonding process.[12,13] It has been demonstrated that FG Al foam with varying pore structures can be fabricated by bonding precursors with different amounts of blowing agent added using FSW, which is carried out prior to the foaming process by heat treatment of the bonded precursor.[14,15] By this FSP route, it has also been demonstrated that FG Al foam with varying alloy composition can be easily fabricated by bonding precursors containing different Al alloys.[16] It is expected that FG Al foam with varying alloy composition exhibiting controlled deformation behavior and compressive properties corresponding to those of each Al alloy in the foam can be realized. In addition, other properties can be realized, for example, corrosion resistance at the surface and high energy absorption in the interior.

In this study, FG Al foam consisting of pure Al (A1050) with high corrosion resistance and Al–Si–Cu alloy (ADC12) with high strength was fabricated by the FSP route. Compression tests were conducted to investigate the compressive response of the A1050–ADC12 FG foam by comparing it with those of uniform A1050 and ADC12 foams.

*Graduate Student, Gunma University

2. Experimental Procedure

Figure 1 shows a schematic illustration of the fabrication process of an A1050–ADC12 FG foam precursor. A1050 pure Al rolled plates and ADC12 (equivalent to A383.0) Al alloy high-pressure die casting plates were used. Some gases are already contained in the die casting plates owing to the die casting process.[17,18] These gases can be used for foaming to fabricate Al foam without using a blowing agent.[19,20] First, as shown in Fig. 1(a), Al plates were stacked with powders distributed between them. A blowing agent (TiH_2, $<45\,\mu m$, 0.6 mass%) and a stabilization agent (α-Al_2O_3, $\sim 1\,\mu m$, 5 mass%) were both used for A1050, and only the stabilization agent was used for ADC12. Second, as shown in Fig. 1(b), multipass FSP[21,22] was applied to obtain a larger amount of precursor and to mix the powders and gases thoroughly. FSP was carried out using a 1D-FSW machine (Hitachi Setsubi Engineering Co., Ltd., Hitachi, Japan). Finally, as shown in Figs. 1(c) and 1(d), both laminated plates were cut in the stirred region and butt-welded by conducting FSW. A precursor was obtained that included the bonding layer as shown in Fig. 1(d).

The precursor was heated in a preheated electric furnace. The holding temperature and holding time were 1003 K and 9.5 min, respectively. Uniform A1050 and ADC12 foams were fabricated by the same process as that used for FG foam. The holding temperature and holding time were 1003 K and 14 min for A1050 and 1003 K and 9.5 min for ADC12, respectively. The difference in the holding time is due to the higher liquidus-line temperature of A1050 (930 K) than ADC12 (853 K) and because the uniform A1050 precursor was not foamed for a holding time of 9.5 min. In contrast, A1050 layer of the FG foam foamed for a holding time of 9.5 min. This is considered to be due to the smaller volume of A1050 of the FG foam than uniform A1050 foam. Clearly, further studies are necessary to optimize the foaming conditions.

The foamed samples were cut by electro-discharge machining, and compression specimens of 20 mm ×

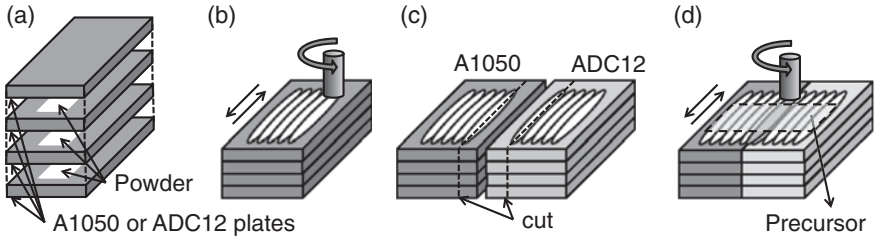

Fig. 1 Schematic illustration of the fabrication process of an A1050–ADC12 FG foam precursor.

20 mm × 40 mm were fabricated. The pore structures in each compression specimen were observed nondestructively by microfocus X-ray CT. Compression tests were carried out at a strain rate of $3.3 \times 10^{-3}\,s^{-1}$.

3. Experimental Results and Discussion

Figure 2 shows the compression test specimens of uniform A1050 foam ($p = 87.3\%$), uniform ADC12 foam ($p = 77.4\%$) and FG ($p = 83.3\%$) foam. The porosity p of these foams was evaluated from mass and dimension measurements. It can be seen that the uniform foams have almost homogeneous pore structures and that the uniform ADC12 foam has smaller pores than the uniform A1050 foam owing to the lower expansion efficiency resulting from not using a blowing agent. In contrast, the FG foam has a pore structure that varies with the position and contains three specific layers, that is, A1050 (upper), transition (middle) and ADC12 (lower) layers.

Figure 3 shows the relationship between the location in the FG foam (in the compression direction), expressed as the height h from the bottom of the specimen normalized by the specimen height, and the porosity p and average pore diameter d_a evaluated from X-ray CT images. It can be seen that the A1050 and ADC12 layers have almost constant porosity and pore diameter, with the A1050 layer having higher values than the ADC12 layer. Note that the porosity and pore diameter became slightly larger in the transition layer, as was also observed in Fig. 2(c). This is considered to be due to the dispersion of the blowing agent during the bonding process shown in Fig. 1(d), which was indicated by the previous studies.[16,23] Namely, the blowing agent, which only existed in the A1050, was dispersed into the ADC12 by the intense stirring action of FSW. During the heating process, the low-melting-point ADC12 first foamed, and the bonding region also foamed before the A1050 because it contained both gases and the blowing agent. The high expansion efficiency of the blowing agent, as shown in the reference,[24] and the earlier occurrence of foaming resulted in the coalescence of pores.

Table 1 shows the porosity and pore diameter of the A1050 and ADC12 layers of the FG foam, along with those of uniform A1050 and ADC12 foams. It can be seen that each layer of the FG foam had almost the same value as that for the uniform foams, although the pore diameter of the A1050 layer of the FG foam was smaller than that for the uniform A1050 foam owing to the longer holding time during the foaming process. The porosity of the foams evaluated from X-ray CT images was lower than that evaluated from mass and dimension measurements. This is mainly due to the procedure used during image processing to clearly observe the pore structures, which involves using a threshold and filtration to distinguish between the aluminum alloy and pores. Also, this is due to the resolution of the X-ray CT images used in this study, in which pores with a diameter below several tens of μm cannot be observed.[25]

Figures 4(a)–4(f) show sequential deformation images of the FG foam. The layer between the two arrows in Fig. 4(a) corresponds to the transition layer indicated in Fig. 3. The FG foam first started to deform in the A1050 layer and the transition layer with high porosity and large pores, and little deformation could be seen in the ADC12 layer up to approximately $\varepsilon = 0.5$; thereafter, the ADC12 layer started to deform. Ordinarily, deformation should first occur in the layer with higher porosity and larger pores. It can be seen from Figs. 4(a)–4(c) that although the transition layer had higher porosity and larger pores than the A1050 layer, the two layers were deformed at almost the same time. This is considered to be because the cell walls in the transition layer were stronger than those in the A1050 layer. This was because the transition layer became a mixture of A1050 and ADC12, resulting in the formation of a high-strength Al–Si alloy due to the stirring action of FSW during the bonding process.[16]

Figure 4(g) shows typical stress–strain curves for the FG foam, along with those of the uniform A1050 and ADC12 foams. To enable the direct comparison of the stress–strain curves between the FG foam and the uniform foams, the nominal strain of the uniform foams was modified, which assumed that the deformation of FG foam at low strain was occurred only in the A1050 layer and the deformation at high strain was occurred only in the ADC12 layer.[14] It was shown that two different plateau regions appeared in the FG foam, which corresponded to the plateau regions appearing in the uniform foams. Table 2 shows the plateau stress of the first and second plateau regions of the FG foam and that of the uniform A1050 and ADC12 foams. The two plateau regions of the FG foam had almost the same plateau stress as that for each corresponding uniform foam. The uniform ADC12 foam had a slightly lower plateau stress than the second plateau stress of the FG foam. This is due to the decrease in stress at the latter of the plateau region. In the uniform ADC12 foam, parts of the cell wall collapsed as a result of local brittle fracture during compression because ADC12 Al alloy is composed of brittle eutectic Al–Si alloy, and the true cross-sectional area decreased.[20] Also, the aspect ratio of the specimen used in this study was comparatively high. In Fig. 4(g) and Table 2, the results for uniform ADC12 foam

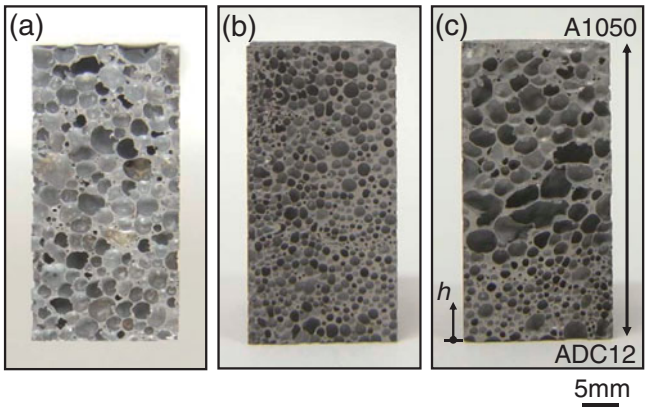

Fig. 2 Compression test specimens of (a) uniform A1050 foam ($p = 87.3\%$), (b) uniform ADC12 foam ($p = 77.4\%$) and (c) A1050–ADC12 FG foam ($p = 83.3\%$).

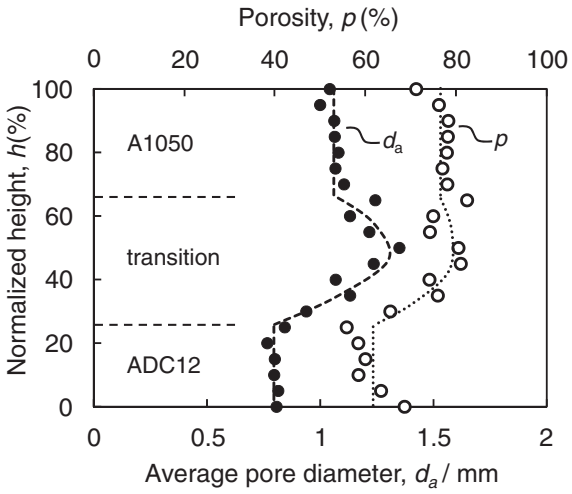

Fig. 3 Relationship between height in the specimen, and porosity and average pore diameter.

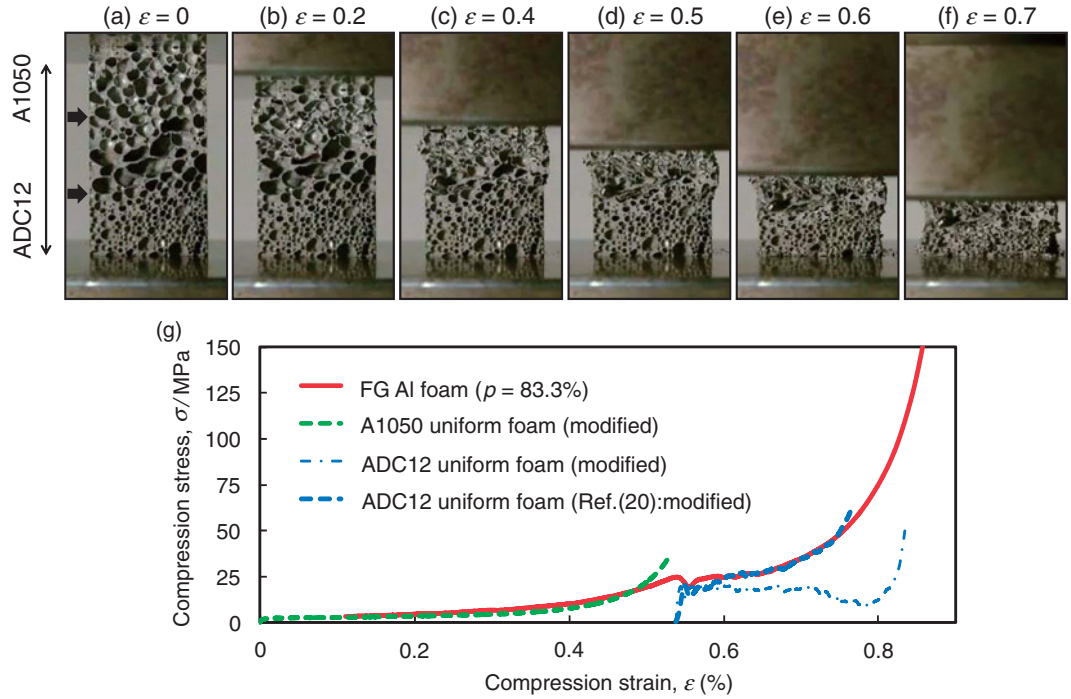

Fig. 4 (a)–(f) Sequential deformation images of FG foam and (g) stress–strain curve of FG foam along with those of uniform A1050 and ADC12 foams.

Table 1 Porosity and pore diameter of A1050 and ADC12 layers of FG foam, along with those of uniform A1050 and ADC12 foams.

	A1050		ADC12	
	FG	Uniform	FG	Uniform
Porosity p (%)	76.7	79.7	61.8	61.5
Average pore diameter d_a/mm	1.06	1.66	0.80	0.84

Table 2 Plateau stress of first and second plateau regions of FG foam and those of uniform A1050 and ADC12 foams.

	A1050		ADC12		
	FG	Uniform	FG	Uniform	Uniform[18]
Plateau stress σ_{pl}/Mpa	3.57	3.26	25.5	18.4	25.9

with a porosity of 76.5% presented in a previous study,[20] which experiment was conducted by the lower aspect ratio of the specimen than the specimen used in this study, are also shown. This foam did not exhibit a decrease in stress during compression tests. It was shown that the uniform ADC12 foam had almost the same plateau stress as the ADC12 layer of the FG foam. From these results, it was shown that the A1050–ADC12 FG foam fabricated by the FSP route had the compression properties of both uniform A1050 and ADC12 foams.

4. Conclusion

In this study, an FG Al foam with varying alloy composition was developed and the compressive properties of the fabricated FG Al foam were demonstrated. It was shown that the A1050–ADC12 FG Al foam has the potential for its location of deformation to be controlled. Moreover, the FG Al foam with plateau regions and stresses corresponding to those of uniform A1050 and ADC12 foams was obtained.

Acknowledgments

This work was financially supported in part by the Industrial Technology Research Grant Program in 2009 from the New Energy and Industrial Technology Development Organization (NEDO) of Japan, the Grant-in-Aid for Young Scientists (B) and by the Light Metal Education Foundation, Inc.

REFERENCES

1) L. J. Gibson: Ann. Rev. Mater. Sci. **30** (2000) 191–227.
2) J. Banhart: Prog. Mater. Sci. **46** (2001) 559–632.
3) A. Pollien, Y. Conde, L. Pambaguian and A. Mortensen: Mater. Sci. Eng. A **404** (2005) 9–18.
4) A. H. Brothers and D. C. Dunand: Adv. Eng. Mater. **8** (2006) 805–809.
5) A. H. Brothers and D. C. Dunand: Mater. Sci. Eng. A **489** (2008) 439–443.
6) K. Huang, D. H. Yang, S. Y. He and D. P. He: J. Phys. D-Appl. Phys. **44** (2011) 365405.
7) A. Hassani, A. Habibolahzadeh and H. Bafti: Mater. Des. **40** (2012) 510–515.
8) S. C. Ferreira, A. Velhinho, R. J. C. Silva and L. A. Rocha: Int. J. Mater. Prod. Technol. **39** (2010) 122–135.
9) K. Shinagawa: Porous Metals and Metallic Foams, ed. by L. P. Lefebvre, J. Banhart and D. C. Dunand, (Destech Pubns Inc., 2008) pp. 95–98.
10) R. Suzuki and K. Kitazono: J. Japan Inst. Metals **72** (2008) 758–762.
11) Y. Hangai, T. Utsunomiya and M. Hasegawa: J. Mater. Process. Technol. **210** (2010) 288–292.
12) R. S. Mishra and Z. Y. Ma: Mater. Sci. Eng. R-Rep. **50** (2005) 1–78.
13) Z. Y. Ma: Metall. Mater. Trans. A **39** (2008) 642–658.
14) Y. Hangai, K. Takahashi, T. Utsunomiya, S. Kitahara, O. Kuwazuru and N. Yoshikawa: Mater. Sci. Eng. A **534** (2012) 716–719.
15) Y. Hangai, K. Takahashi, R. Yamaguchi, T. Utsunomiya, S. Kitahara, O. Kuwazuru and N. Yoshikawa: Mater. Sci. Eng. A **556** (2012) 678–684.
16) Y. Hangai, Y. Oba, S. Koyama and T. Utsunomiya: Metall. Mater. Trans. A **42** (2011) 3585–3589.
17) D. F. Allsop and D. Kennedy: *Pressure Diecasting, Part 2, The Technology of the Casting and the Die*, (Pergamon Press, Ltd., New York, 1983) pp. 6–7.
18) W. Walkington: *Gas Porosity: A Guide to Correcting the Problems*, (North American Die Casting Association, Illinois, 2006).
19) Y. Hangai, H. Kato, T. Utsunomiya and S. Kitahara: Metall. Mater. Trans. A **41** (2010) 1883–1886.
20) Y. Hangai, H. Kato, T. Utsunomiya, S. Kitahara, O. Kuwazuru and N. Yoshikawa: Mater. Trans. **53** (2012) 1515–1520.
21) Y. S. Sato, S. H. C. Park, A. Matsunaga, A. Honda and H. Kokawa: J. Mater. Sci. **40** (2005) 637–642.
22) J. Q. Su, T. W. Nelson and C. J. Sterling: Scr. Mater. **52** (2005) 135–140.
23) Y. Hangai, S. Koyama, T. Utsunomiya and M. Hasegawa: J. Japan Inst. Metals **74** (2010) 285–287.
24) T. Utsunomiya, K. Takahashi, Y. Hangai and S. Kitahara: Mater. Trans. **52** (2011) 1263–1268.
25) Y. Hangai, S. Maruhashi, S. Kitahara, O. Kuwazuru and N. Yoshikawa: Metall. Mater. Trans. A **40** (2009) 2789–2793.